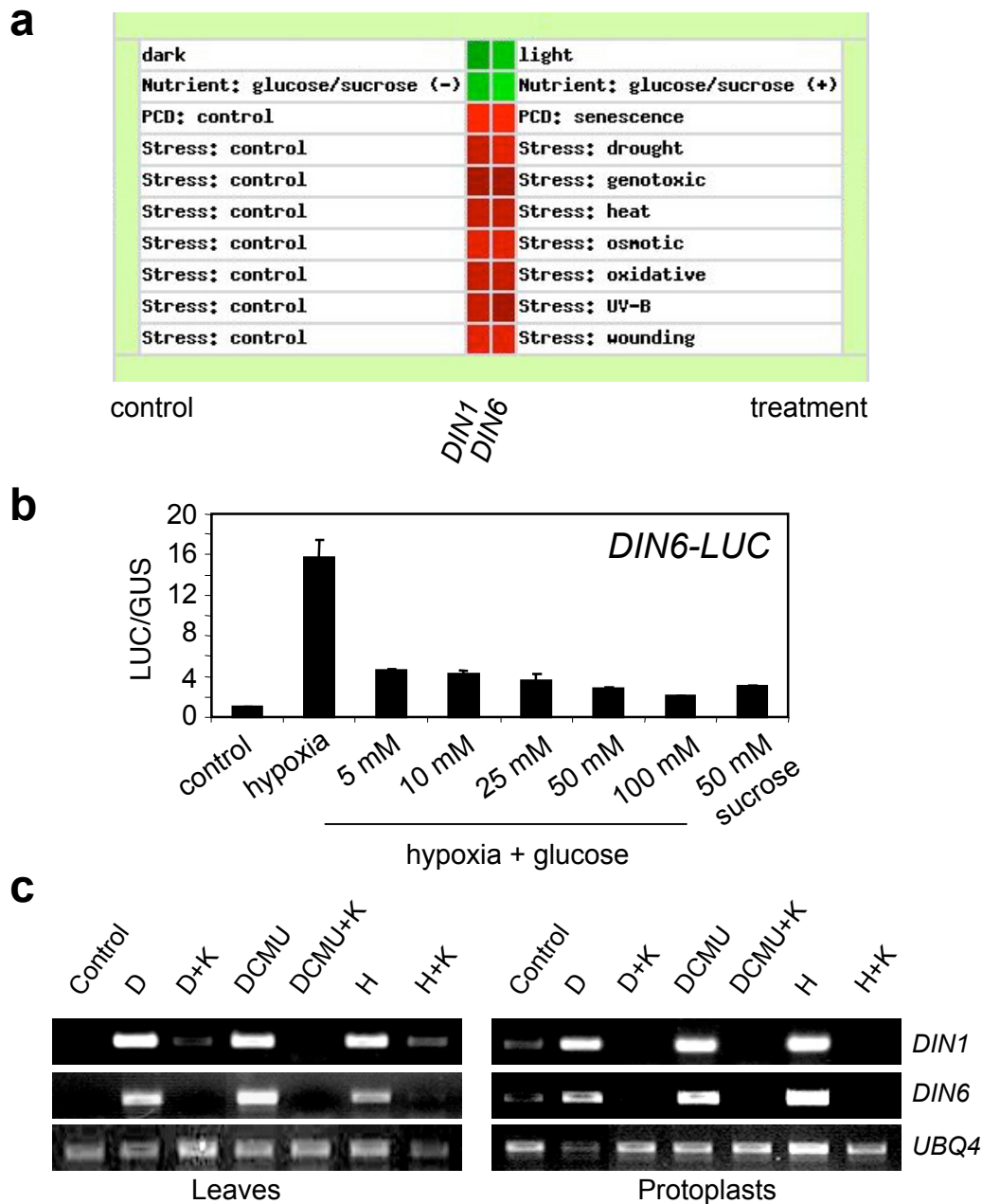
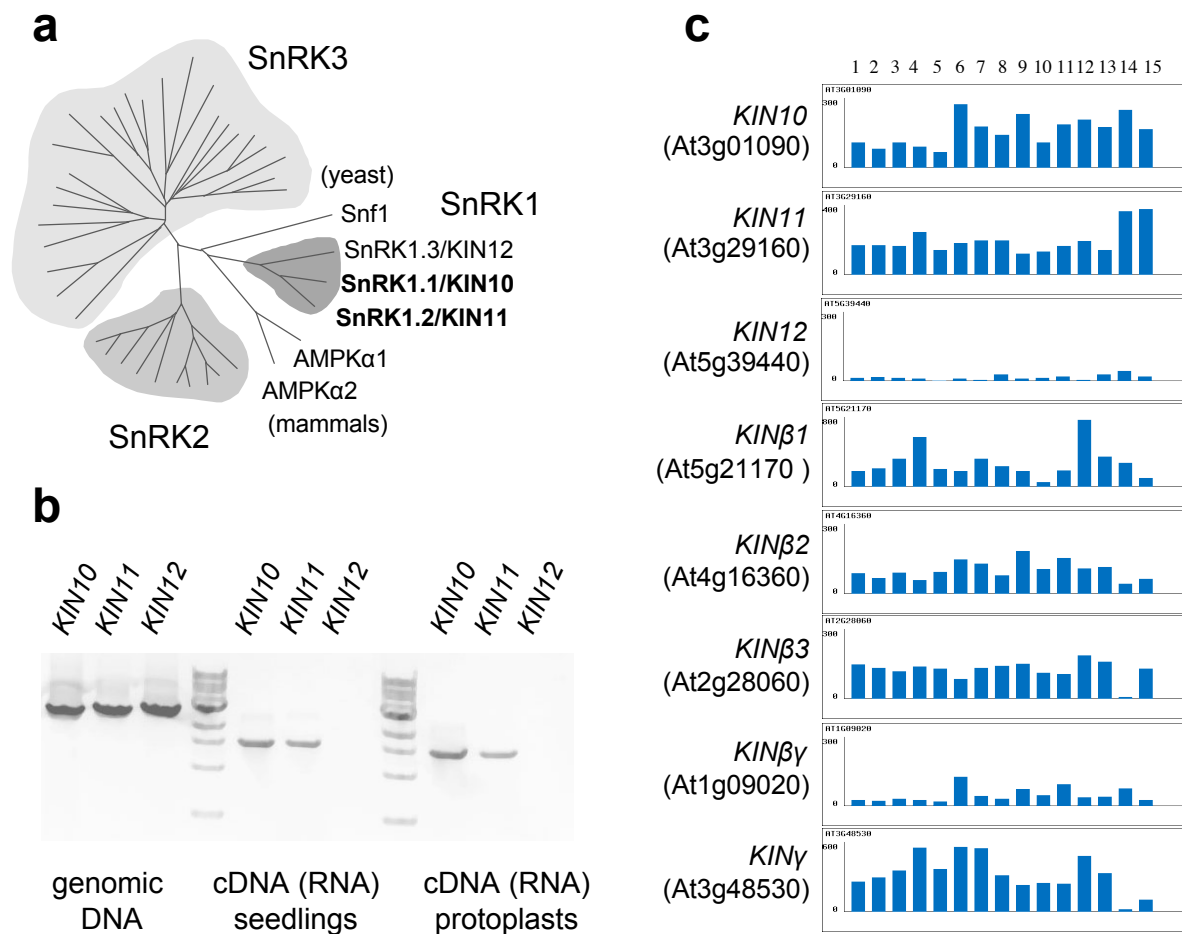


**Supplementary Figure 1 | KIN10/11 are central integrators of sugar, metabolic, stress, and developmental signals** (see next page for Figure Legend)

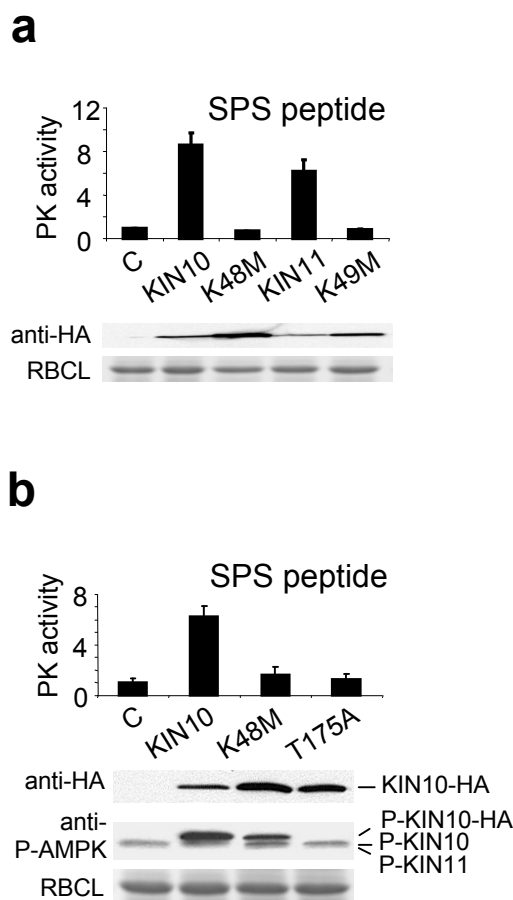
**Supplementary Figure 1 | KIN10/11 are central integrators of sugar, metabolic, stress, and developmental signals.** Plants are constantly challenged by multiple types of stress that ultimately converge as an energy-deficiency signal in the cell, triggering the activation of KIN10/11. Conversely, sugars have a repressive effect, and at least in autotrophic tissues both glucose and sucrose inhibit KIN10/11 action even when the stress factors persist. Upstream protein kinases (PKs), protein phosphatases<sup>1</sup>(PPs), and additional regulatory subunits<sup>2-6</sup> may contribute to the fine-tuning of the system and possibly confer tissue and cell-type specificity. Activated KIN10/11 initiates an energy-saving program at several levels, aiming at repressing biosynthetic pathways and at promoting catabolic processes and photosynthesis to increase ATP generation. KIN10/11 directly and indirectly regulates key metabolic enzymes to inhibit specific assimilation pathways<sup>7-9</sup>. Remarkably, KIN10/11 regulation involves massive transcriptional reprogramming that affects a wide range of both plant-specific and evolutionarily conserved pathways. This is partly mediated by the S-class of bZIP transcription factors. In addition to contributing to the maintenance of cellular energy homeostasis and tolerance to (nutrient) stress, KIN10/11 have profound effects at the whole organism level influencing growth, viability, reproduction and senescence. KIN10/11 seem to be the convergence point linking multiple metabolic, stress and developmental signals, thus playing a fundamental and highly conserved role in vegetative and reproductive growth and survival. NR, nitrate reductase; SPS, sucrose phosphate synthase; HMG-CoAR, 3-hydroxy-3-methylglutaryl-coenzyme A reductase.



**Supplementary Figure 2 | Regulation of *DIN6* expression.** **a**, *DIN1* and *DIN6* are repressed by light and sugar but induced by multiple types of stress<sup>10-19</sup>. The data were obtained by using the microarray database mining tool (Meta-Analyzer) provided by Genevestigator<sup>20</sup>. **b**, *DIN6-LUC* induction by hypoxia is repressed by glucose and sucrose. Error bars indicate standard deviations from three independent experiments. **c**, The PK inhibitor K252a (K) inhibits the induction of *DIN* gene expression by darkness and stress. D, dark; H, hypoxia. Control, DCMU and hypoxia treatments were performed under light.



**Supplementary Figure 3 | Expression patterns of *Arabidopsis* genes encoding the putative catalytic and regulatory subunits of SnRK1. a**, The *Arabidopsis* SnRK superfamily comprises 3 groups. The SnRK1s are most homologous to yeast Snf1 and mammalian AMPK. **b**, RT-PCR analyses. *KIN10* and *KIN11*, but not *KIN12* are expressed in *Arabidopsis* seedlings and mesophyll protoplasts. **c**, Expression of the catalytic subunit genes, *KIN10*, *KIN11*, *KIN12* and the genes encoding putative regulatory subunits ( $\alpha$ ,  $\beta$ ,  $\gamma$ ,  $\beta\gamma$ )<sup>2-5</sup> in the indicated plant materials and treatments. Without co-expression of  $\beta$  and  $\gamma$  regulatory subunits, an overexpressed mammalian AMPK catalytic  $\alpha$  subunit was inactive and degraded<sup>21</sup>. Possibly, plant-specific regulation<sup>22,23</sup> or/and sufficient endogenous regulatory  $\beta$  and  $\gamma$  proteins were present to support their activities when *KIN10/11* were overexpressed in leaf cells. The data were obtained from the gene expression search program provided by the *Arabidopsis* Membrane Protein Library (AMPL, <http://www.cbs.umn.edu/arabidopsis/>). 1, whole plant; 2, whole plant, ozone-treated; 3, whole plant, constant light; 4, whole plant, constant light, water treated; 5, whole plant, constant light, glc treated; 6, primary roots, 1% suc; 7, lateral roots; 8, lateral roots, nematode infection; 9, shoots; 10, shoots, treated at 4°C; 11, petioles; 12, active axillary buds; 13, dormant axillary buds; 14, mature pollen; 15, suspension cells.



**Supplementary Figure 4 | KIN10 and KIN11 are active kinases.** **a**, KIN10 and KIN11 expressed in protoplasts displayed the characteristic and conserved ability of SnRK1 to phosphorylate a specific peptide substrate (RDHMPRIRSEMQUIWSED) derived from sucrose phosphate synthase (SPS)<sup>24,25</sup>. K48M and K49M are inactive KIN10 and KIN11 mutant controls, respectively. **b**, Phosphorylation of T175 is essential for KIN10 activity. KIN10 and KIN11 phosphorylated at the conserved T175<sup>26</sup> are recognised by an antibody against phosphorylated and activated mammalian AMPK on T172 (anti-P-AMPK). KIN10 is probably phosphorylated by endogenous upstream kinase(s)<sup>21</sup>, but reduced phosphorylation levels of K48M suggest also autophosphorylation. Total recombinant KIN10 and KIN11 were detected with an anti-HA antibody. RBCL coomassie staining served as endogenous protein control. P-KIN10, KIN10 phosphorylated at T175; C, control DNA. Error bars indicate standard deviations (n=3).

***DIN6* PROMOTER SEQUENCE**

(-624)

TGTATTCACTTTCTGATAAAATGCTAATCCTACAATCAAATGCAAGTGGTTCC

ACCATTGTCGTGATAACACGTGTACGGCTCTAAAGCAATCAGAACAATCATT  
T T  
G2 D3

GGACAGTTTTTACACCGTCAGATAAGTACCTATCCACTTGCTGACTCAGCCG  
T  
T

GATAAACCCCTAAACCGGAAGTTTGCCCCACCGTCAAATTGGAAGAAACCG

GACAAAAGAGAATGTAAAGACTAAGAAGTAAGAACCCATCGGACGTCGTAA  
T T A  
D2 D1 C

GAAGGTTAATTACACGTGGAAACAGCTGGTCAGAGTTATCCGGTAACTTAT  
T A  
G1

CCGGTTACAAGTAAAAAATAATTTGTTCCCATACACGACTCCTTCAGAACC

AAACGCGACATCACGGCGCCGTTTAGTGTCT**TATA**AATAGAGCAATCGGTCCG

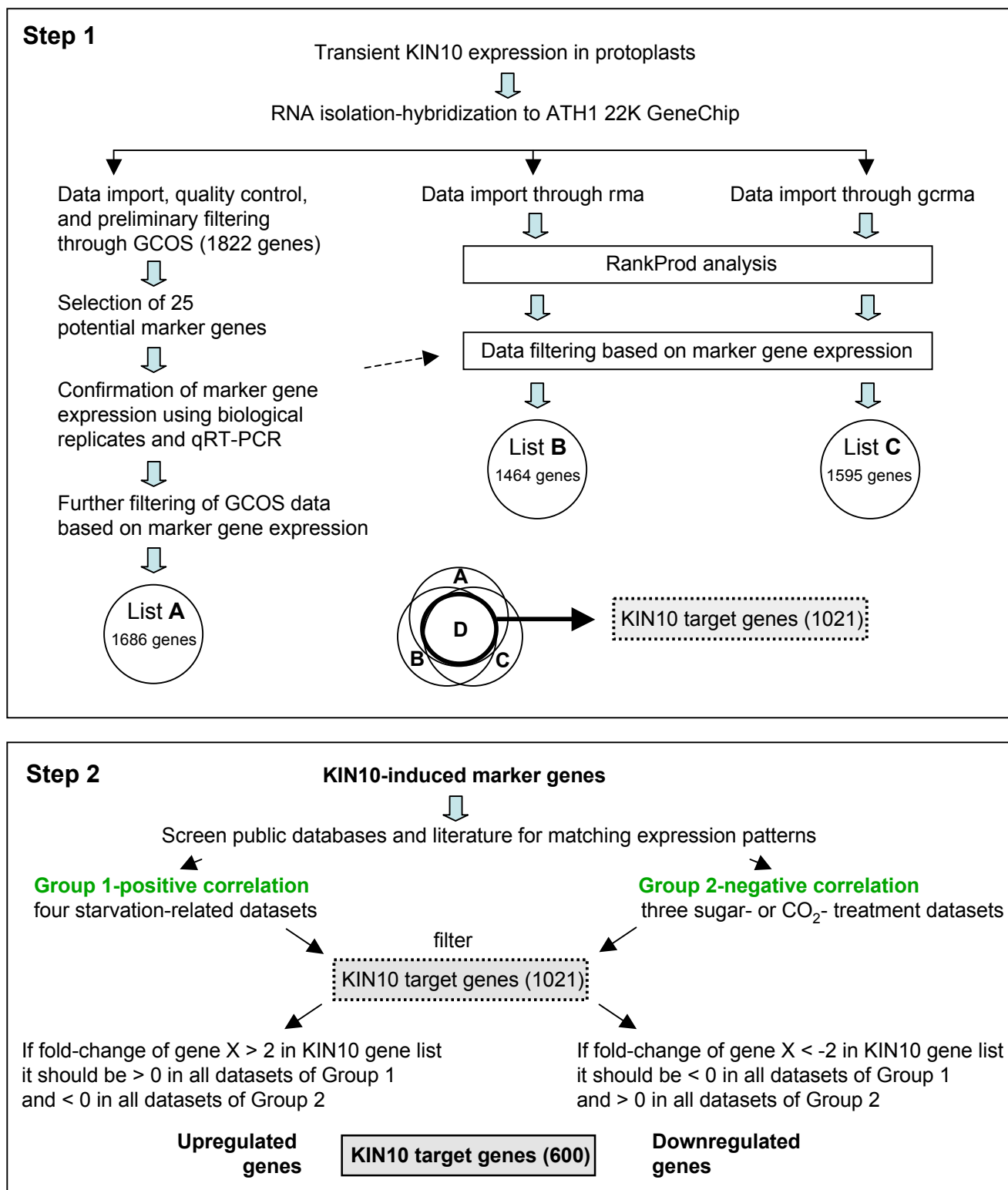
TAGAAAACCAAGACATCAAAAACACGAATATCGATAGTACACTTCTACGTGC

AATTTTCTCCTTTCTCTTCTGGACATCTGTCTGTTTATTACATTTTCTTGTA

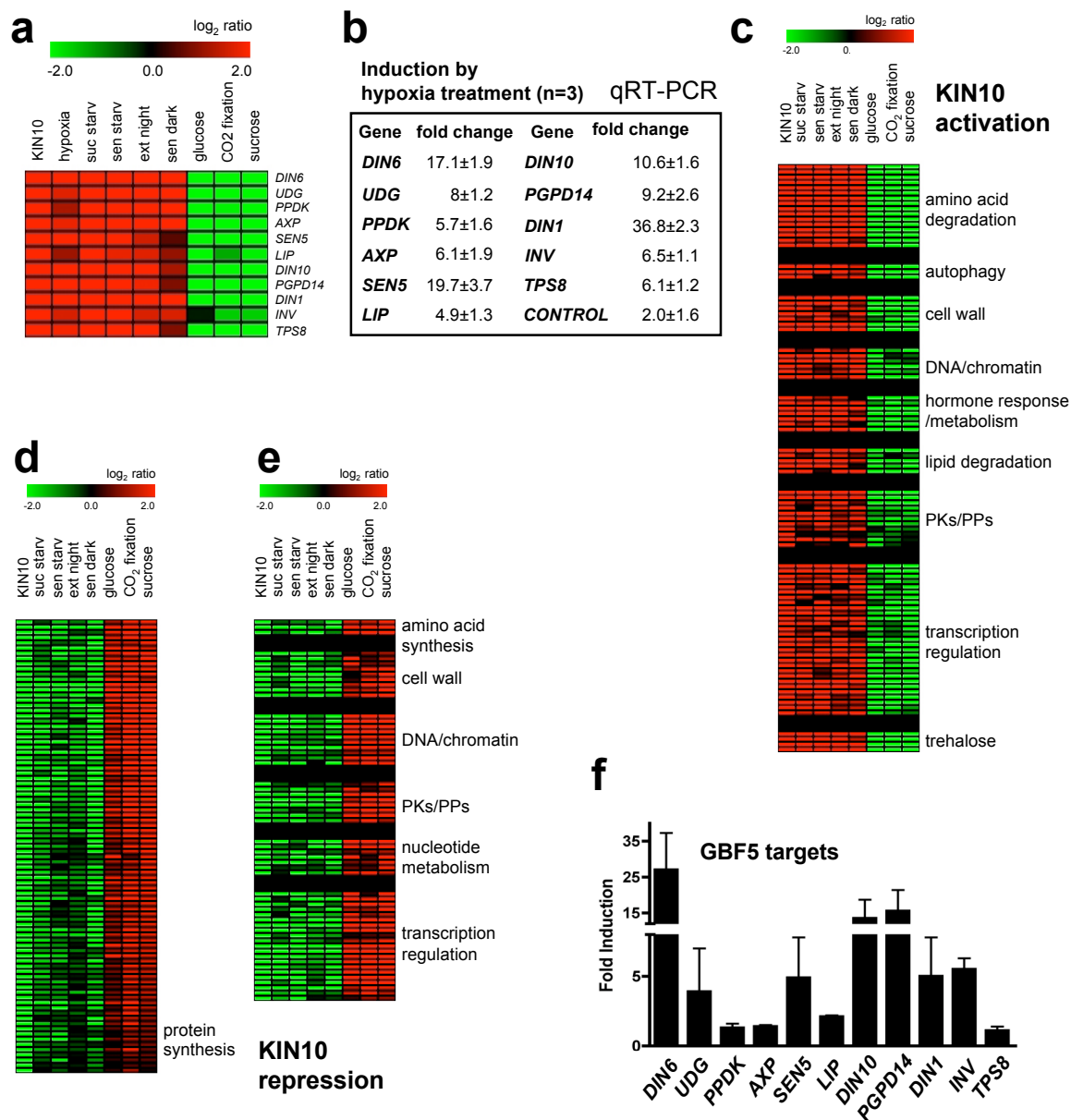
TCTCTTTTGGGGTTTTACAATATCTATCCCCTAAAGTTTCGGAAAATTCTGT

TTTTCTGTTCTCATTCTTCGTGATCTTTTCACTTTCTTCAAAAAAAAAC **ATG**

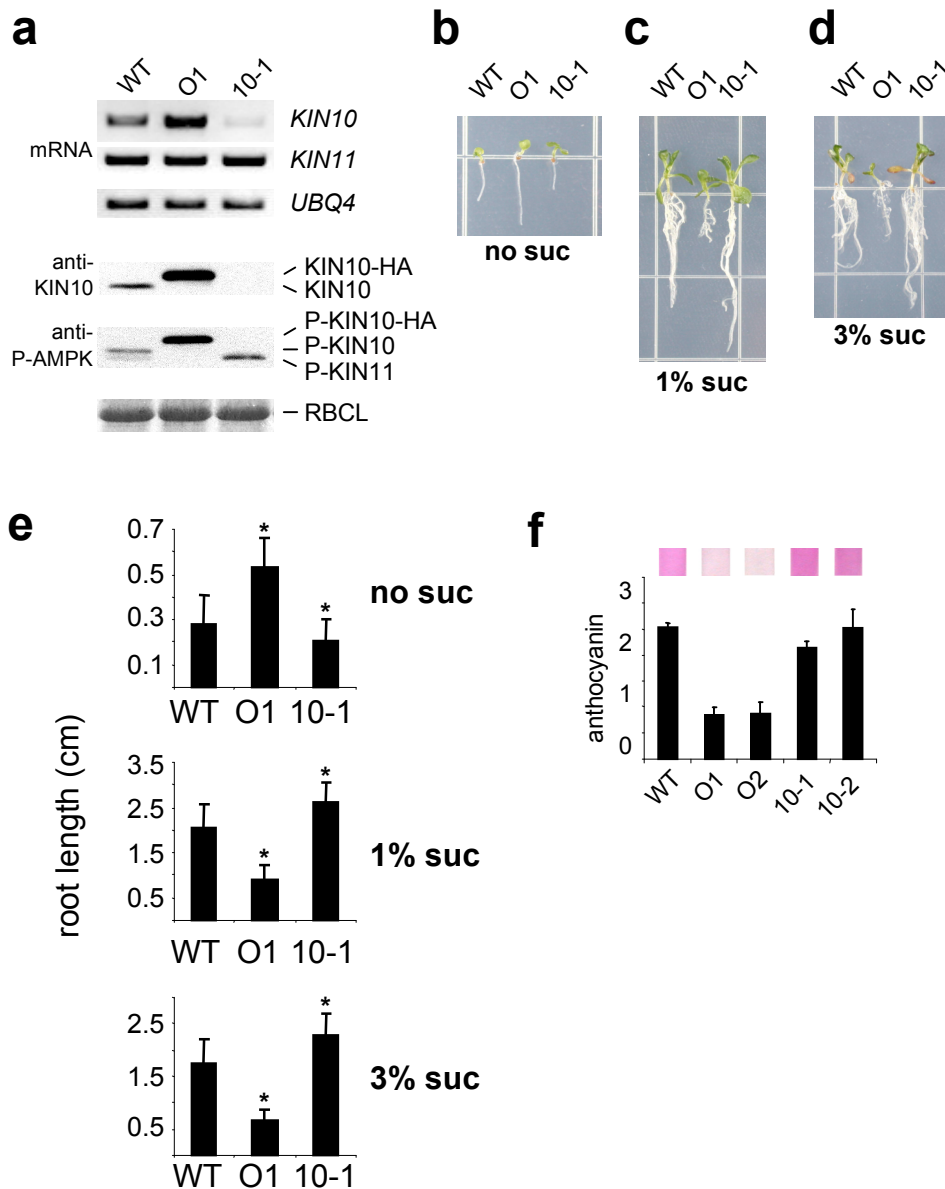
**Supplementary Figure 5 | Regulation of *DIN6* expression.** *DIN6* promoter sequences and selected putative regulatory *cis*-elements (in red and underlined)<sup>27</sup>. Mutated nucleotides are in bold. G1 and G2 represent G-box elements (CACGTG); C a C-box element (GACGTC). Both are bound by bZIP TFs<sup>28-30</sup>. D1, D2 and D3 indicate DOF TF binding sites (A/TAAAG). Plant-specific DOF TFs mediate stress, light and hormone signaling and control carbon and nitrogen metabolism<sup>31,32</sup>. T indicates the TATCCA element, together with the G-box isolated as an essential element of a sugar response sequence (SRS) required for expression of a rice  $\alpha$ -amylase gene under starvation conditions<sup>33</sup>. The TATA-box and start codon are in bold, the leader sequence in blue.



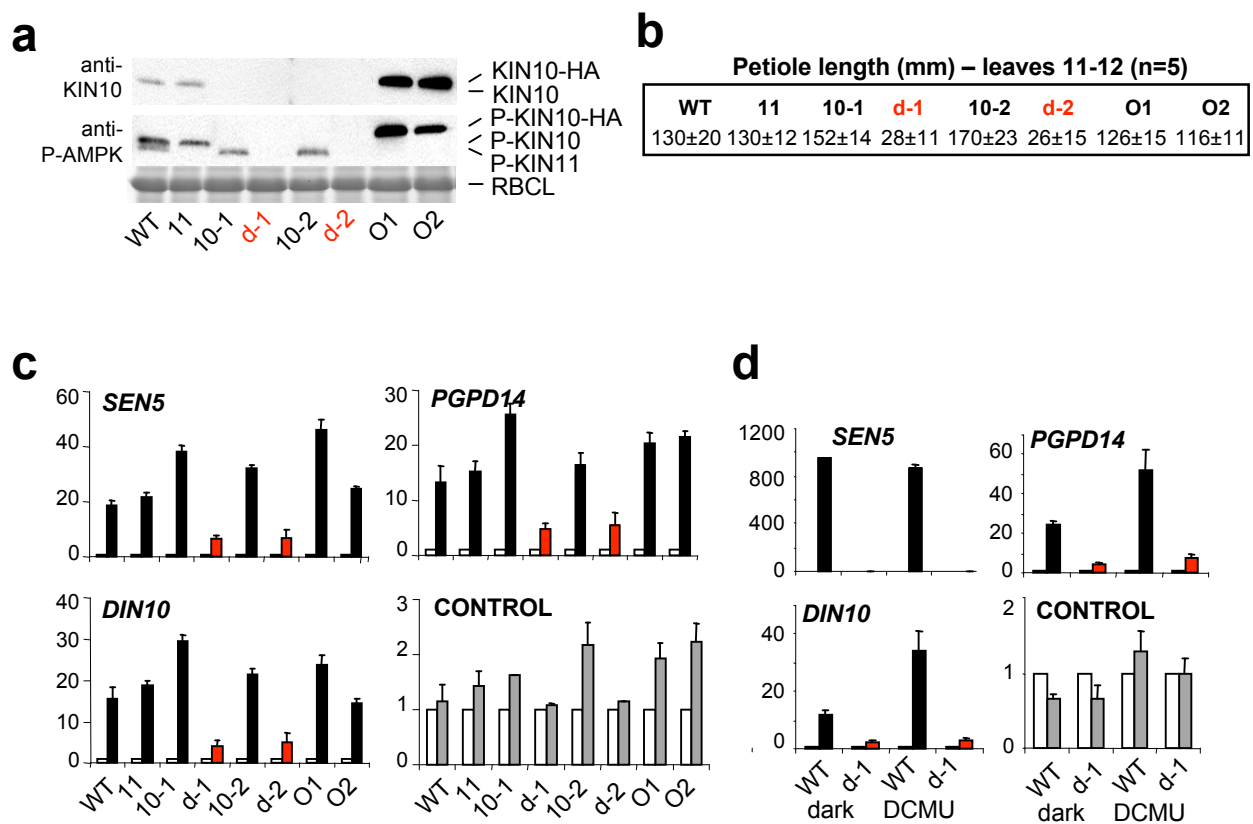
Supplementary Figure 6 | Definition of KIN10 target genes. Filtering strategy outline.



**Supplementary Figure 7 | Global gene expression regulation by KIN10.** **a**, Selected KIN10 marker genes are activated by hypoxia and other types of cellular energy stress. **b**, Analysis of hypoxia induction of KIN10 marker genes (Supplementary Table 2a) by qRT-PCR. **c-e**, Transient *KIN10* expression in protoplasts results in the induction (**c**) and repression (**d**, **e**) of genes involved in a wide variety of cellular processes and metabolism. **f**, GBF5 induces expression of endogenous KIN10 target genes. ext: extended; sen: senescence; starv: starvation; suc: sucrose, PK: protein kinase; PP: protein phosphatase. Error bars indicate standard deviations (n=3).



**Supplementary Figure 8 | Overexpression of KIN10 affects plant development, senescence and starvation responses.** **a**, *KIN10* overexpression (O1) and silencing (10-1) in transgenic plants were examined by RT-PCR and immunoblotting with anti-KIN10 and anti-P-AMPK antibodies. Epitope-tagged transgenic KIN10-HA and endogenous KIN10 protein levels were detected with a KIN10-specific antibody. P-KIN10-HA represented the major phosphorylated form in the overexpression lines. *KIN10* overexpression stimulates growth in the absence of exogenous sugar (**b**, **e**), but reduces growth promotion by 1-3% sucrose (**c**, **d**, **e**). *KIN10* overexpression prevents sucrose-induced anthocyanin accumulation (**e**) Error bars indicate standard deviations (e,  $n > 60$ ; f,  $n = 3$ ). Asterisks indicate statistically significant differences ( $p < 0.05$ ).



**Supplementary Figure 9 | *KIN10/11* silencing results in altered morphology and disrupts transcriptional activation by stress.** **a**, WT, *KIN10* overexpression (O1, O2), *kin10* RNAi (10-1, 10-2), *kin11* VIGS (11) and the *kin10 kin11* VIGS double mutant (d-1, d-2) plants were similarly infiltrated with a control GFP or a *KIN11* construct in the viral vector and examined after 3 weeks using anti-*KIN10* and anti-P-AMPK antibodies. **b**, The double mutants exhibit a dramatic reduction in petiole length. **c-d**, The *KIN10* target gene response to various stresses is abolished in the *kin10 kin11* double mutants. Gene expression was measured by qRT-PCR (see Supplementary Table 2a for gene annotation details and Supplementary Table 6 for other genes and numeric values) from hypoxia-treated mesophyll cells (**c**) and dark- or DCMU-treated leaves (**d**). Control, DCMU, and hypoxia treatments were performed under light. Error bars indicate standard deviations (**c**, n=3; **d**, n=2).

## SUPPLEMENTARY TABLES

### **Supplementary Table 1 (Microsoft Excel file). Global gene expression regulation**

**by KIN10 and hypoxic conditions. Raw data.** Gene expression changes induced by 6h of transient KIN10 expression or hypoxia treatment in *Arabidopsis* protoplasts. Eight  $\mu\text{g}$  of total RNA was used for labeling and hybridization on 22K ATH1 *Arabidopsis* GeneChips®. The data were compiled and normalized using the GCOS v. 1.0 software. The document contains an Excel file with original unfiltered data from two biologically independent replicates of the KIN10 experiment and one hypoxia experiment.

### **Supplementary Table 2. Experimental validation of selected KIN10 marker genes**

**by quantitative real time PCR (qRT-PCR).** Twenty five putative KIN10 marker genes covering diverse functional categories were selected based on their high (100-fold) or moderate (3-fold) transcriptional changes upon KIN10 expression, as revealed in the GeneChip® experiments described in Supplementary Table 1 (see Supplementary Methods for details). Their expression changes were confirmed by two independent protoplast transfection experiments and qRT-PCR analysis.

Supplementary Table 2 (cont.) a, Induced KIN10 marker genes

Gene	Functional category	Annotation	Fold change
<i>DIN6</i> At3g47340	amino acid metabolism	glutamine-dependent asparagine synthetase <u>dark inducible 6</u>	256±1.2
<i>LIP</i> At5g18630	lipid metabolism	triacylglycerol <u>lipase</u> -like protein	12.1±1.1
<i>PPDK</i> At4g15530	gluconeogenesis amino acid metabolism	pyruvate-orthophosphate <u>dikinase</u>	9.8±1.9
<i>INV</i> At1g12240	sucrose metabolism	<u>vacuolar invertase</u>	90.5±1.7
<i>DIN10</i> At5g20250	minor CHO metabolism	raffinose synthase family <u>dark inducible 10</u>	36.8±1.9
<i>TPS8</i> At1g70290	trehalose metabolism	<u>trehalose-6-phosphate synthase</u> , putative	13±1.6
<i>UDG</i> At1g12780	cell wall	<u>uridine diphosphate glucose epimerase</u>	39.4±1.5
<i>PGPD14</i> At5g22920	RNA regulation	pollen germination related protein PGPD14	194±1.3
<i>DIN1</i> At4g35770	RNA regulation	<u>senescence-associated protein 1</u>	256±3.2
<i>SEN5</i> At3g15450	hormone response/ signaling.auxin	<u>senescence-associated protein 5</u>	256±1.7
<i>AXP</i> At2g33830	hormone signaling auxin	putative <u>auxin-regulated protein</u>	238.9±1.1

Supplementary Table 2 (cont.) b, Repressed KIN10 marker genes.

Gene	Functional category	Annotation	Fold change
<i>EXP10</i> At1g26770	cell wall	cell wall modification <u>expansin</u> 10	-31.6±1.6
<i>DWF4</i> At3g50660	hormone metabolism brassinosteroid	steroid 22-alpha-hydroxylase <u>dwarf4</u>	-6.3±1.0
<i>JMT</i> At1g19640	hormone metabolism jasmonate	jasmonic acid carboxyl <u>methyltransferase</u>	-11.2±1.3
<i>AAPI</i> At1g58360	transport	<u>amino acid permease</u> I	-5.7±1.2
<i>MDR1</i> At2g36910	transport	putative ABC transporter <u>multidrug resistance</u>	-6.9±1.2
<i>SUR1</i> At2g20610	hormone metabolism auxin	IAA biosynthesis <u>SUPERROOT</u> 1	-3.6±1.4
<i>ADK1</i> At3g09820	nucleotide metabolism salvage	<u>Adenosine Kinase</u> 1	-5.2±1.2
<i>HDT1</i> At3g44750	RNA transcription regulation	<u>Histone deacetylase</u> HD2 family	-11.6±1.2
<i>IFL1</i> At5g60690	RNA transcription regulation	<u>interfascicular fiberless</u> 1 REVOLUTA transcription factor	-4.7±1.7
<i>MYB30</i> At3g28910	RNA transcription regulation	MYB30 transcription factor	-5.6±1.0
<i>MYB75</i> At1g56650	RNA transcription regulation/anthocyanin synthesis	MYB75 transcription factor	-4.2±1.0
<i>DPS</i> At3g21500	secondary metabolism. isoprenoids	putative 1-D- <u>deoxyxylulose</u> 5- <u>phosphate synthase</u>	-12.8±1.4
<i>L34</i> At3g28900	protein synthesis	60S ribosomal protein <u>L34</u>	-8.2±1.2
<i>L37</i> At1g15250	protein synthesis	60S ribosomal protein <u>L37</u>	-3.1±1.7

**Supplementary Table 3 (Microsoft Excel file). Global gene expression regulation by KIN10. Filtered data.** Duplicated KIN10 vs. control microarray data were subjected to three independent layers of filtering: *i*) GCOS-imported data were filtered based on the Affymetrix presence (P) or absence (A) call, a two-fold change cut-off, and a change call *p*-value cutoff of  $<0.0004$ ; *ii*) rma-normalized RankProd<sup>34</sup> data and *iii*) gcrma-normalized RankProd data were filtered based on a two-fold change and a *p*-value cutoff of  $<0.012$  (see Supplementary Methods and Supplementary Fig. 6 for details). Only the overlapping genes from all three filtered lists (*i-iii*) were considered as KIN10 target genes for presentation here. Assignment to specific functional categories was mainly based on the classification in the MapMan program<sup>12</sup> and annotated using combined information from TIGR and publications. The annotation file and the transcription factor nomenclature used are available on the Sheen lab website. Values are the average of the two independent replicates. Genes shown in italics are present in duplicate to allow visualization in two functional categories.

**Supplementary Table 4 (Microsoft Excel file). The transcriptional program induced by KIN10 markedly overlaps with that induced by starvation conditions and is antagonized by increased sugar availability.** The genes listed in Supplementary Table 3 were subjected to more stringent filtering by comparing their expression to published microarray datasets where sugar and carbon starvation was induced by various treatments<sup>10-13</sup> or where sugar levels were increased by differential CO<sub>2</sub> fixation or exogenous sugar<sup>14-16</sup>. Only genes complying with the following criteria were kept and are presented in this table: *i*) if the fold-change of gene X > 2 in the KIN10 gene list, it should be > 0 in all starvation-related datasets and < 0 in all the sugar and CO<sub>2</sub> datasets, *ii*) if the fold-change of gene X < -2 in the KIN10 gene list, it should be < 0 in all starvation-related datasets and > 0 in all the sugar and CO<sub>2</sub> datasets. These genes were used for the graphic comparisons shown in Fig. 3. KIN10 average: average values of the two independent KIN10 experiments; SUC STARV, cultured cells after 24 h sucrose starvation<sup>10</sup>; SEN STARV, starvation-induced senescence<sup>11</sup>; EXT NIGHT, extended night resulting in carbon deprivation<sup>12</sup>; SEN DARK, darkness-induced senescence<sup>13</sup>, 1 day; GLUCOSE, 3% glucose addition (3h in the dark) to 24 h-starved seedlings<sup>14</sup>; CO<sub>2</sub> FIXATION, 4h-treatment of plants with low [CO<sub>2</sub>] (<50 ppm) vs. ambient [CO<sub>2</sub>] (350 ppm)<sup>15</sup>; SUCROSE, 1% sucrose addition (8h 70 μE light) to 48h-starved seedlings<sup>16</sup>. See Supplementary Methods and Supplementary Fig. 6 for detailed information on selected datasets and filtering strategy. Functional classification of genes and annotation are as in Supplementary Table 3.

**Supplementary Table 5. Pair-wise correlations between KIN10 target genes in the KIN10 and starvation-related or sugar-supplementation microarray experiments.**

Pearson correlation coefficients confirm the reproducibility of the KIN10 target gene response and its extensive positive and negative correlation with changes induced upon starvation, and sugar supplementation or differential CO<sub>2</sub> fixation, respectively. The correlation coefficient of KIN10 replicates was calculated from the GCOS-imported and filtered subset of genes (1822) (see Supplementary Fig. 6). All other correlations were calculated from the subset of genes (600) described in Supplementary Table 4. SEN DEV1, developmental senescence<sup>11</sup>; SEN DEV2, developmental senescence, AtGenExpress<sup>11</sup>; other datasets are as in Supplementary Table 4.

<b>condition</b>	<b>correlation coefficient with KIN10</b>
KIN10 REPLICATES	0.94
SUC STARV	0.87
SEN STARV	0.86
SEN DARK	0.85
EXT NIGHT	0.85
SEN DEV1	0.35
SEN DEV2	0.31
GLUCOSE	-0.87
CO <sub>2</sub> FIXATION	-0.88
SUCROSE	-0.92

**Supplementary Table 6. Quantitative RT-PCR analyses of KIN10 target genes activated by hypoxia.** Fold-induction by hypoxia treatment of protoplasts from the indicated plants is shown. All plants were similarly infiltrated with a GFP control or KIN11 construct in the viral vector and examined after 3 weeks using anti-KIN10 and anti-P-AMPK antibodies. WT; *11*: *kin11*(VIGS); *10-1* and *10-2*: *kin10*(RNAi); *d-1* and *d-2*: *kin10 kin11*(VIGS) double mutants, *O1* and *O2*: *KIN10* overexpression lines; control (gene): *CIPK23* expression. The results are depicted graphically for the indicated genes in Fig. 4g and Supplementary Fig. 9c. Errors are from duplicated samples (n=2) or indicate standard deviations (n=3). (n)= number of replicates of independent experiments.

	WT (3)	<i>11</i> (3)	<i>10-1</i> (2)	<i>d-1</i> (2)	<i>10-2</i> (3)	<i>d-2</i> (3)	<i>O1</i> (3)	<i>O2</i> (2)
<i>DIN6</i>	21.86±5.5	22.16±2.2	57.68±2.8	3.03±1.9	35.51±2.3	2.22±3.7	46.21±2.1	56.89±1.5
<i>LIP</i>	2.22±1.5	2.58±1.2	4.23±1.4	1.11±1.0	3.18±1.6	1.06±1.9	5.588±1.3	3.73±1.2
<i>PPDK</i>	3.36±1.9	3.53±1.5	6.28±1.2	(-1.19±1.3)	4.76±1.6	1.89±1.5	7.89±1.8	4.53±1.1
<i>INV</i>	2.89±1.1	3.92±1.6	4±1.6	(-1.11±1.1)	4.99±1.1	1.39±1.5	5.94±2.7	4.08±1.7
<i>DIN10</i>	15.67±2.7	18.77±1.7	29.45±1.7	4.08±1.3	21.41±1.6	4.86±2.5	23.75±2.3	14.42±1.3
<i>UDG</i>	2.58±1.6	2.69±1.5	4.29±1.0	(-1.15±1.0)	4.2±1.5	(-1.17±2.2)	4.69±1.6	3.86±1.3
<i>PGPD14</i>	13.27±3.0	15.14±1.9	25.63±2.0	4.86±1.0	16.56±2.2	5.46±2.3	20.39±2.0	21.56±1.0
<i>DIN1</i>	8.46±2.1	16.8±1.3	23.92±2.2	3.03±1.1	20.82±1.4	2.6±2.9	21.11±1.2	13.45±1.9
<i>SEN5</i>	18.64±1.9	21.86±1.6	38.05±2.5	6.5±1.2	32±1.3	6.82±3.3	45.89±3.9	24.76±1.0
<i>AXP</i>	4.59±1.5	4.86±1.2	10.2±1.0	(-1.02±1.0)	5.78±1.3	1.93±1.1	8.69±1.7	7.73±1.2
<i>control</i>	1.1±0.3	1.4±0.3	1.6±0	1.1±0	2.2±0.4	1.1±0.0	1.9±0.3	2.2±0.3

**Supplementary Table 7 (Microsoft Excel file). Sequences of primers used in this study.**

## SUPPLEMENTARY METHODS

### Global gene expression analyses.

A graphical overview of the data import and filtering process is presented in Supplementary Fig. 6.

**1. MIAME (Minimal Information About Microarray Experiments):** For global gene expression analyses, about 3 million protoplasts were isolated from the fifth and sixth leaves of 36 plants (4 weeks old) and pooled for two large transfection experiments (scaled up 50-fold). Cells ( $1.5 \times 10^6$ ) were transfected with 1mg of control or *KIN10*-expressing plasmid DNA and incubated in 10 ml mannitol buffer in a 150 x 15 mm Petri dish for 6h. The incubation time for transfected protoplasts was experimentally determined to cover early gene expression (0.5-3h) in response to diverse signals in protoplasts (JS, unpublished). For hypoxia treatment, cells ( $1.5 \times 10^6$ ) were incubated in 2 ml buffer in a 15 ml Falcon tube (25 mm depth) for 6h. To maximize the significance of the duplicated experimental data for defining differentially expressed genes, the biologically independent experiments were carefully performed by two individuals using different soil, plants, growth chambers, DNAs and microarray facilities for hybridization and scanning to cover potential technical and biological variations. The hypoxia GeneChip® experiment was carried out once for confirmation purpose. Total RNA was extracted using Trizol® (Invitrogen) and about 8 µg was labeled for hybridization using standard Affymetrix protocols and *Arabidopsis* ATH1 GeneChips® containing 22,810 probe sets<sup>35</sup> (Affymetrix, Santa Clara, CA). Hybridization and scanning were performed at the Brigham and Women's Hospital Microarray Facility (Boston, MA) and Harvard Medical School-Partners Healthcare Center for Genomic Research (Cambridge, MA).

Affymetrix GeneChip® Operating Software (GCOS v. 1.0) and Bioconductor<sup>36</sup> packages, *affy*, *affyPLM*, *rma*, *gcrma*, *limma*, and *RankProd*, were downloaded (<http://www.bioconductor.org/>) and used for standard quality controls, normalization and data analyses. The original GeneChip® files will be available at TAIR (The Arabidopsis Information Resource).

**2. Data analysis using Affymetrix GCOS.** Transcript expression values from scanned arrays were first analyzed using GCOS, and were subjected to global scaling using a target value of 1500 (as recommended by Affymetrix, Supplementary Table 1). The percentage of genes called “present” in a single hybridization ranged from 57-61%. Preliminary filtering was performed based on the Affymetrix presence (P) or absence (A) call and two-fold increase or decrease change ( $\log_2$  ratio of 1 or -1, respectively) between samples expressing *KIN10* vs. control plasmid DNA. The following categories were filtered out using Excel: *i*) probe sets called “A” in both the control and treatment, *ii*) probe sets called “P” for the control, “A” for the treatment, but “increased” or “mildly increased” for the change, *iii*) probe sets called “A” for the control, “P” for the treatment but “decreased” or “mildly-decreased” for the change, *iv*) probe sets called “not changed”, *v*) probe sets called “decreased”, but having positive  $\log_2$  ratios, *vi*) probe sets called “increased”, but having negative  $\log_2$  ratios. The high reproducibility of the duplicated datasets was reflected by a high correlation coefficient of 0.94 for the 1822 filtered genes.

**3. Selection of marker genes and experimental validation.** For experimental validation of the potentially up and down-regulated genes by *KIN10* based on the analysis using GCOS, 25 marker genes covering diverse functional categories were selected with high

(100-fold) and moderate (3-fold) log<sub>2</sub> ratios with low *p*-value ( $p < 0.0004$ ). Duplicated protoplast transfection experiments and real time qRT-PCR analysis were carried out independently to confirm that all 25 genes are truly activated or repressed by KIN10 (Supplementary Tables 2, 3), similar to the duplicated GeneChip® datasets. Using the *p*-value cutoff of the experimentally validated marker genes ( $p < 0.0004$ ), an additional filtering step was applied to the GCOS data (log<sub>2</sub> ratio of 1 or -1), which yielded a list of 1686 genes (Supplementary Fig. 6).

**4. Statistical analysis of putative KIN10 target genes using RankProd<sup>34</sup>.** To identify system-wide KIN10 target genes, we performed statistical analysis of the duplicated datasets using the parametric linear model (limma) and the nonparametric RankProd packages available in Bioconductor. The Bioconductor programs, affy, affyPLM, rma and gcrma, were used to perform GeneChip® normalization before running limma and RankProd algorithms. Based on the 25 experimentally validated marker genes, it was obvious that the linear model performed poorly as nearly half of the experimentally validated marker genes were not selected using even a relatively high *p*-value cut-off (0.02). On the contrary, the non-parametric RankProd analysis covered all 25 marker genes based on similar *p*-value cut-off (0.02) using either rma or gcrma for data normalization. The statistic method provided *p*-value and false discovery rate (FDR) values to help define the differentially expressed gene candidates. A list of putative KIN10 target genes were thereby selected based on the stringent overlap of results from GCOS analysis described above and RankProd(rma) and RankProd(gcrma) using the *p*-value cut-off (0.012) of the validated *MYB75*<sup>37</sup> marker gene instead of an arbitrary *p*-value or FDR cut-off (Supplementary Table 2). However, the high selection stringency

likely generated false negatives. There were 1021 genes (506 increased and 515 decreased) with essential functions in diverse regulatory and metabolic pathways (Supplementary Table 3; Supplementary Fig. 6).

**5. Stringent selection of KIN10 target genes by positive and negative correlations with global gene expression profiles.** To increase the robustness and explore the physiological significance of the KIN10 target genes, we used the experimentally and statistically validated marker genes to screen the ATH1 databases and literature for positively and negatively correlated gene expression profiles. We identified 4 experiments (Group 1: sugar starvation, sugar depletion-induced senescence, darkness, extended night) and 3 treatments (Group 2: glucose, sucrose and ambient CO<sub>2</sub> vs compensation point CO<sub>2</sub>) that display remarkable positively and negatively correlated gene expression profiles, respectively. The datasets identified as positively correlating with the KIN10 dataset are: SUC STARV, cultured cells after 24h sucrose starvation<sup>10</sup>; SEN STARV, starvation-induced senescence, NASCArray<sup>38</sup> experiment number 30<sup>11</sup>; EXT NIGHT, extended night resulting in carbon deprivation<sup>12</sup>; SEN DARK, darkness-induced senescence, 1 day<sup>13</sup>; the datasets identified as negatively correlating with the KIN10 dataset are: GLUCOSE, 3% glucose addition (3h in the dark) to 24h-starved seedlings<sup>14</sup>; CO<sub>2</sub> FIXATION, differential induction of endogenous sugar levels by 4h-treatment of plants under low [CO<sub>2</sub>] (<50 ppm) vs. ambient [CO<sub>2</sub>] (350 ppm)<sup>15</sup>; SUCROSE, 1% sucrose addition (8h, 70 μE light) to 48h-starved seedlings<sup>16</sup>.

Based on our hypothesis that KIN10 might be engaged in the transcriptional response to sugar and energy starvation, an additional filtering step was applied to the 1021 previously identified KIN10 target genes and only those complying with the

following criteria were kept: *i*) if the fold-change of gene  $x > 2$  in the KIN10 gene list, it should be  $> 0$  in all datasets of group 1 and  $< 0$  in all datasets of group 2, *ii*) if the fold-change of gene  $x < -2$  in the KIN10 gene list, it should be  $< 0$  in datasets of group 1 and  $> 0$  in all datasets of group 2. This final filtering step yielded a list of 278 induced and 322 repressed genes. Hierarchical clustering analysis (with Euclidean distance) of the KIN10 target genes was performed with the TIGR MeV program<sup>39</sup> before (data not shown) and after filtering to visualize their relationship and regulation in the eight conditions and treatments (Figs 3a, 3b). The full gene lists are provided in Supplementary Table 4. Pearson correlation coefficients were calculated in Excel for this subset of genes to demonstrate their close relationship to the KIN10 dataset (Supplementary Table 5). As a negative control, correlation coefficients were also calculated for a set of 600 randomly selected genes. Two datasets for the transcriptional profile of developmental senescence (SEN DEV1 and SEN DEV2<sup>11</sup>) were also used for the calculation of Pearson correlation coefficients.

**6. Hypoxia induction of gene expression.** To further test the hypothesis that KIN10 might be engaged in the transcriptional response to sugar and energy starvation, we performed a comparison of the genes induced by KIN10 and the various starvation conditions described above (Supplementary Table 4) and the genes induced in our hypoxia ATH1 GeneChip® experiment (Supplementary Table 1). The overlap of the expression profiles was confirmed by triplicated qRT-PCR analyses of selected marker genes (Supplementary Fig. 7a, b).

**7. Functional classification and annotation.** Genes were classified according to the MapMan program functional categories<sup>12</sup> with some modifications for the cell, cell wall,

hormone metabolism, major carbohydrate metabolism, metal handling, protein, RNA, and signalling categories (Supplementary Tables 3, 4), and annotated using combined information from TIGR and publications. The annotation file and the transcription factor nomenclature used are available on the Sheen lab web site ([http://genetics.mgh.harvard.edu/sheenweb/search\\_affy.html](http://genetics.mgh.harvard.edu/sheenweb/search_affy.html)).

### Supplementary references

1. Fordham-Skelton, A.P., *et al.* A novel higher plant protein tyrosine phosphatase interacts with SNF1-related protein kinases via a KIS (kinase interaction sequence) domain. *Plant J.* **29**, 705-715 (2002).
2. Bouly, J.P., Gissot, L., Lessard, P., Kreis, M., & Thomas, M. *Arabidopsis thaliana* proteins related to the yeast SIP and SNF4 interact with AKINalpha1, an SNF1-like protein kinase. *Plant J.* **18**, 541-550 (1999).
3. Ferrando, A., Koncz-Kalman, Z., Farras, R., Tiburcio, A., Schell, J., & Koncz, C. Detection of *in vivo* protein interactions between Snf1-related kinase subunits with intron-tagged epitope-labelling in plants cells. *Nucleic Acids Res.* **29**, 3685-3693 (2001).
4. Lumbreras, V., Alba, M.M., Kleinow, T., Koncz, C., & Pages, M. Domain fusion between SNF1-related kinase subunits during plant evolution. *EMBO Rep.* **2**, 55-60 (2001).
5. Gissot, L., Polge, C., Bouly, J.P., Lemaitre, T., Kreis, M., & Thomas, M. AKINbeta3, a plant specific SnRK1 protein, is lacking domains present in yeast and mammals non-catalytic beta-subunits. *Plant Mol. Biol.* **56**, 747-759 (2004).
6. Bhalerao, R. P. *et al.* Regulatory interaction of PRL1 WD protein with *Arabidopsis* SNF1-like protein kinases. *Proc. Natl Acad. Sci. USA* **96**, 5322-5327 (1999).
7. Kaiser, W.M. & Huber S. C. Post-translational regulation of nitrate reductase: Mechanism, physiological relevance and environmental triggers. *J. Exp. Bot.* **52**, 1981-1989 (2001).

8. Sugden, C., Donaghy, P. G., Halford, N. G. & Hardie, D. G. Two SNF1-related protein kinases from spinach leaf phosphorylate and inactivate 3-hydroxy-3-methylglutaryl-coenzyme A reductase, nitrate reductase, and sucrose phosphate synthase *in vitro*. *Plant Physiol.* **120**, 257-274 (1999).
9. Halford, N. G. *et al.* Metabolic signalling and carbon partitioning: role of Snf1-related (SnRK1) protein kinase. *J. Exp. Bot.* **54**, 467-475 (2003).
10. Contento, A. L., Kim, S. J. & Bassham, D. C. Transcriptome profiling of the response of Arabidopsis suspension culture cells to Suc starvation. *Plant Physiol.* **135**, 2330-2347 (2004).
11. Buchanan-Wollaston, V. *et al.* Comparative transcriptome analysis reveals significant differences in gene expression and signalling pathways between developmental and dark/starvation-induced senescence in Arabidopsis. *Plant J.* **42**, 567-585 (2005).
12. Thimm, O. *et al.* MAPMAN: a user-driven tool to display genomics data sets onto diagrams of metabolic pathways and other biological processes. *Plant J.* **37**, 914-39 (2004).
13. Lin, J. F. & Wu, S. H. Molecular events in senescing Arabidopsis leaves. *Plant J.* **39**, 612-628 (2004).
14. Price, J., Laxmi, A., St Martin, S. K. & Jang, J. C. Global transcription profiling reveals multiple sugar signal transduction mechanisms in Arabidopsis. *Plant Cell* **16**, 2128-2150 (2004).
15. Bläsing, O.E. *et al.* Sugars and circadian regulation make major contributions to the global regulation of diurnal gene expression in Arabidopsis. *Plant Cell* **17**,

- 3257-3281 (2005).
16. Palenchar, P.M., Kouranov, A., Lejay, L.V. & Coruzzi, G.M. Genome-wide patterns of carbon and nitrogen regulation of gene expression validate the combined carbon and nitrogen (CN)-signaling hypothesis in plants. *Genome Biol.* **5**, R91(2004)
  17. Lam, H.M., Coschigano, K.T., Oliveira, I.C., Melo-Oliveira, R. & Coruzzi GM. The molecular genetics of nitrogen assimilation into amino acids in higher plants. *Annu. Rev. Plant Physiol. Plant Mol. Biol.* **47**, 569-593 (1996).
  18. Lam, H. M., Hsieh, M. H. & Coruzzi, G. Reciprocal regulation of distinct asparagine synthetase genes by light and metabolites in *Arabidopsis thaliana*. *Plant J.* **16**, 345-353 (1998).
  19. Fujiki, Y. *et al.* Dark-inducible genes from *Arabidopsis thaliana* are associated with leaf senescence and repressed by sugars. *Physiol. Plant.* **111**, 345-352 (2001).
  20. Zimmermann, P., Hirsch-Hoffmann, M., Hennig, L. & Gruissem, W. GENEVESTIGATOR. Arabidopsis Microarray Database and Analysis Toolbox. *Plant Physiol.* **136**, 2621-2632 (2004).
  21. Kahn, B. B., Alquier, T., Carling, D. & Hardie, D. G. AMP-activated protein kinase: ancient energy gauge provides clues to modern understanding of metabolism. *Cell Metab.* **1**, 15-25 (2005).
  22. Sugden, C., Crawford, R. M., Halford, N. G. & Hardie, D. G. Regulation of spinach SNF1-related (SnRK1) kinases by protein kinases and phosphatases is

- associated with phosphorylation of the T loop and is regulated by 5'-AMP. *Plant J.* **19**, 433-439 (1999).
23. Toroser, D., Plaut, Z. & Huber, S. C. Regulation of a plant SNF1-related protein kinase by glucose-6-phosphate. *Plant Physiol.* **123**, 403-412 (2000).
  24. Sugden, C., Donaghy, P. G., Halford, N. G. & Hardie, D. G. Two SNF1-related protein kinases from spinach leaf phosphorylate and inactivate 3-hydroxy-3-methylglutaryl-coenzyme A reductase, nitrate reductase, and sucrose phosphate synthase *in vitro*. *Plant Physiol.* **120**, 257-274 (1999).
  25. Huang, J. Z. & Huber, S. C. Phosphorylation of synthetic peptides by a CDPK and plant SNF1-related protein kinase. Influence of proline and basic amino acid residues at selected positions. *Plant Cell Physiol.* **42**, 1079-1087 (2001).
  26. Hardie, D. G., Carling, D. & Carlson, M. The AMP-activated/SNF1 protein kinase subfamily: metabolic sensors of the eukaryotic cell? *Annu. Rev. Biochem.* **67**, 821-855 (1998).
  27. Steffens, N. O., Galuschka, C., Schindler, M., Bulow, L. & Hehl, R. AthaMap web tools for database-assisted identification of combinatorial *cis*-regulatory elements and the display of highly conserved transcription factor binding sites in *Arabidopsis thaliana*. *Nucleic Acids Res.* **33**, W397-402 (2005).
  28. Foster, R., Izawa, T., & Chua, N.H. Plant bZIP proteins gather at ACGT elements. *FASEB J.* **8**, 192-200 (1994).
  29. Menkens, A.E., Schindler, U., & Cashmore, A.R. The G-box: a ubiquitous regulatory DNA element in plants bound by the GBF family of bZIP proteins. *Trends Biochem. Sci.* **20**, 506-510 (1995).

30. Jakoby, M. *et al.* bZIP transcription factors in Arabidopsis. *Trends Plant Sci.* **7**, 106-111 (2002).
31. Yanagisawa, S., Akiyama, A., Kisaka, H., Uchimiya, H. & Miwa, T. Metabolic engineering with Dof1 transcription factor in plants: Improved nitrogen assimilation and growth under low-nitrogen conditions. *Proc. Natl. Acad. Sci. USA* **101**, 7833-7838 (2004).
32. Yanagisawa, S. Dof domain proteins: plant-specific transcription factors associated with diverse phenomena unique to plants. *Plant Cell Physiol.* **45**, 386-391 (2004).
33. Lu, C. A., Lim, E. K. & Yu, S. M. Sugar response sequence in the promoter of a rice alpha-amylase gene serves as a transcriptional enhancer. *J. Biol. Chem.* **273**, 10120-10131 (1998).
34. Breitling, R., Armengaud, P., Amtmann, A., & Herzyk, P. Rank Products: A simple, yet powerful, new method to detect differentially regulated genes in replicated microarray experiments, *FEBS Lett.* **573**, 83-92 (2004).
35. Redman, J.C., Haas, B.J., Tanimoto, G. & Town, C.D. Development and evaluation of an *Arabidopsis* whole genome Affymetrix probe array. *Plant J.* **38**, 545-61 (2004).
36. Gentleman, R.C., *et al.* Bioconductor: open software development for computational biology and bioinformatics. *Genome Biol.* **5**, R80 (2004).
37. Borevitz, J. O., Xia, Y., Blount, J., Dixon, R. A. & Lamb, C. Activation tagging identifies a conserved MYB regulator of phenylpropanoid biosynthesis. *Plant Cell* **12**, 2383-2394 (2000).

38. Craigon, D.J., James, N., Okyere, J., Higgins, J., Jotham, J., & May, S. NASCArrays: A repository for Microarray Data generated by NASC's Transcriptomics Service. *Nuc. Acids Res.* **32**, D575-D577 (2004).
39. Saeed, A. I. *et al.* TM4: a free, open-source system for microarray data management and analysis. *Biotechniques* **34**, 374-378 (2003).